Template Design and Propagation Gain for Multipath UWB Channels with Per-Path Frequency-Dependent Distortion.

Neil Mehta, Alexandra Duel-Hallen and Hans Hallen
North Carolina State University
Email: {nbmehta2, sasha, hans_hallen}@ncsu.edu

ABSTRACT

Due to the large bandwidth allocation, Ultra-Wideband (UWB) channels exhibit frequency-dependent distortion of individual multipath components. This per-path distortion is particularly significant in outdoor UWB applications, where line-of-sight (LOS) or non-distorted reflected signals might not be available at the receiver, and the dominant propagation mechanisms involve shadowing (diffraction) or reflection by small objects (e.g. signs or lamp-posts). In this paper, a physical model is employed in the design of robust correlation receiver templates for outdoor single and multipath impulse radio channels characterized by per-path distortion. It is demonstrated that receivers which employ a set of partial derivatives templates are near-optimal in terms of energy capture while the simple transmit pulse template provides excellent complexity-performance trade-offs for most practical scenarios. Moreover, iterative receiver structures that maintain the energy capture in the receiver for overlapping components are investigated. Finally, a large gap between the propagation gains of the transmit pulses in the lower and upper bands of the FCC spectrum is characterized for several propagation mechanisms, and implications for adaptive UWB transmissions are discussed.[*]

I. INTRODUCTION

Ultra wideband (UWB) impulse radio [1] is a wireless technology involving transmission of very short duration pulses on the order of nanoseconds. It is defined by FCC [2] as any wireless transmission scheme that possesses a fractional bandwidth $W/f_c > 20\%$, where W is the transmission bandwidth and f_c is the center frequency, or a -10 dB bandwidth greater than 500 MHz regardless of the fractional bandwidth of the system. The FCC spectral masks released in 2002 [2] allow the use of 0~0.96 GHz and 3.1~10.6 GHz bands on an unlicensed basis subject to certain restrictions on the signal power spectrum density (PSD).

Due to the very large bandwidth allocation for UWB systems, individual multipath components at the receiver undergo frequency dependent per-path distortion through reflection from small objects, shadowing (diffraction), penetration through walls, etc. Template design for distorted UWB channels was investigated in [3,4]. These methods employ basis expansion and are computationally complex. To reduce complexity, we propose to take into account physical channel characteristics in the receiver design.

Physics-based studies on UWB pulse distortion have been reported in [5,6], where the diffracted pulse is derived directly from expressions of the Uniform Theory of Diffraction (UTD) and Geometry Theory of Diffraction (GTD). Moreover, a physical model for outdoor UWB channels was developed in [7] and was used to investigate the frequency-dependent behavior of per-path distortion in single-path UWB channels with diffraction and reflection as dominant outdoor propagation conditions. This model is based on a Fresnel diffraction augmentation of the method of images [8,9,10]. It provides a more accurate description of the dependency of strength and shape of the received pulse on position in given local environment. Based on this study, we propose approximate per-path templates generated by fractional differentiation and integration of the transmit pulse, which effectively model the frequency-dependent behavior of UWB channels characterized by reflection from small reflectors and diffraction, respectively. These propagation mechanisms are often dominant in outdoor UWB channels [7]. We examine complexity-performance tradeoffs for correlation receivers which employ a set of these templates in terms of energy capture for several Gaussian monocycle transmit pulses. Moreover, we identify worst case and beneficial scenarios for utilization of simple transmit pulse template.

We also address correlation receiver design for UWB systems with pulse overlap at the receiver, or inter-pulse interference (IPI). Although the pulse width of UWB systems is on the order of nanoseconds, the assumption that multipath components are clearly resolvable is not always realistic [11,12]. In this paper, we demonstrate that a simple iterative receiver employed in [3] is suitable for diverse multipath scenarios affected by IPI and frequency-dependent distortion.

Finally, we analyze and compare the frequency-dependent propagation gains of Gaussian monocycle pulses in the upper and lower bands of the FCC spectral mask [2] for multipath UWB channels affected by different propagation mechanisms. Adaptive transmission techniques where the transmit pulse that resides in one of the bands is selected when the channel is strong in that part of the spectrum are discussed.

[*] This research was supported by NSF grant ECCS-0809612.

The rest of this paper is organized as follows. In section II, we discuss the UWB system model and receiver design. In section III, template design for single path UWB channels characterized by per-path distortion due to diffraction or reflection from small reflectors is investigated. In section IV, we address iterative receiver design for overlapping multipath components and extend receiver design to realistic multipath channels with per-path distortion, with focus on complexity/performance tradeoffs for proposed templates. Propagation gain analysis for multipath channels and possible implications on adaptive transmission are discussed in section V.

II. UWB System Model and Receiver Design

The multipath UWB channel impulse response can be modeled as

$$h(t) = \sum_{k=1}^{L} h_k(t-\tau_k) \ , \qquad (1)$$

where L is the total number of paths, $h_k(t)$ is the impulse response and τ_k is the propagation delay of the k^{th} multipath component, respectively [13]. The received signal is given by the convolution of the channel impulse response with the transmit signal $p_t(t)$ and can be represented by:

$$p_r(t) = \sum_{k=1}^{L} p_r^{(k)}(t-\tau_k) + n(t) \ , \qquad (2)$$

where $p_r^{(k)}(t) = h_k(t) * p_t(t)$ is the received pulse waveform associated with the k^{th} path, $n(t)$ is zero-mean, Additive White Gaussian Noise (AWGN) random process with double-sided power spectrum density $N_0/2$, and '*' denotes convolution. To simplify timing estimation and to isolate the impact of per-path distortion, the effects of the additive noise on the receiver design are ignored in the paper.

In typical UWB channels, the received signal contains many multipath components [14]. Each of these components corresponds to a path affected by certain propagation mechanism. The transmitted signal is detected by collecting the energy associated with dominant (strongest) multipath components using the RAKE receiver. Each finger of the RAKE receiver is given by a matched filter/correlation receiver [1,15]. The correlation template signal

$$v(t) = \sum_{k=1}^{L'} v_k(t-\hat{\tau}_k) \ , \qquad (3)$$

is the sum of individual per-path templates $v_k(t)$, $1 \le k \le L'$ (referred to as the "templates" in the remainder of the paper), each delayed by time of arrival estimate $\hat{\tau}_k$. We assume that $v(t)$ is normalized to unit energy. Suppose the L multipath components in (2) do not overlap (pulse overlap will be addressed in Section IV). Denote the energy of the received pulse as $E_r = \int_{-\infty}^{\infty} p_r^2(t)dt$. Then the peak of the cross-correlation between the received pulse and the correlation template (3) is [16]:

$$\rho = \sum_{k=1}^{L'} \int_{-\infty}^{\infty} p_r^{(k)}(t-\tau_k) v_k(t-\hat{\tau}_k) dt \Big/ \sqrt{E_r} \ , \qquad (4)$$

where the peak of the cross-correlation for each individual path is achieved at $\hat{\tau}_k$. The parameter ρ in (4) plays a key role in the performance of the correlation detector. When the k^{th} path is not distorted, the optimum template for that path is the normalized transmit pulse $p_t(t)$, while the optimum template choice for any received path is $v_k(t) = p_r^{(k)}(t)/\sqrt{E_r}$, and the corresponding maximum value of $\rho = 1$. However, $\rho < 1$ if the template is not matched to the channel response, resulting in reduced energy capture [3]. In this paper, this loss is characterized by the SNR capture

$$SNR_c = \rho^2 \ (\text{dB}) \ , \qquad (5)$$

We employ Gaussian monocycle transmit pulses, which are frequently adopted in UWB systems [14,17]. The n^{th} order Gaussian monocycle pulse is defined as:

$$w_n(t) = \frac{d^n}{dt^n}\left(e^{-2\pi(t/t_p)^2}\right) \ , \qquad (6)$$

where t_p is a parameter that controls the bandwidth of the pulse, and n corresponds to the shift in the 'mode frequency' of the spectrum, or the peak of the PSD, given by $f_m = \sqrt{n}\,\frac{1}{t_p\sqrt{\pi}}$ [16]. Fig. 1(a) shows the power spectral densities (PSD) of several Gaussian monocycle pulses and the FCC spectral mask, and Fig. 1(b) illustrates a 2^{nd} order Gaussian monocycle waveform. Note that the 2^{nd} order pulse (t_p=2.5ns) and the 8^{th} order pulse (t_p=0.25ns) have mode frequencies of 0.34 GHz and 6.5 GHz and reside in the lower (0-0.96 GHz) and upper (3.1-10.6 GHz) bands of the FCC spectral mask, respectively. Fig. 1(a) also illustrates the PSD of the 2^{nd} order Gaussian monocycle pulse with t_p=0.25ns. While this pulse does not fit the spectral mask, it is often used in the literature on pulse and template design [18,19]. In this paper, we employ the 2^{nd} order Gaussian monocycle pulses with t_p=0.25ns and 2.5ns to illustrate the worst case frequency-dependent distortion.

III. Template Design for Single-Path Channels with Distortion

The frequency responses of simulated UWB channel are obtained using our physical model [7]. The sample

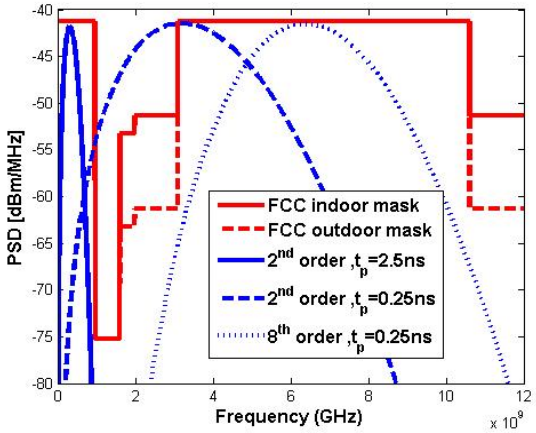

(a)

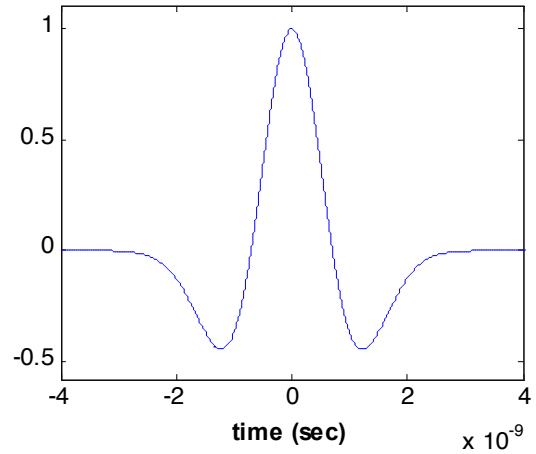

(b)

Figure 1. a) PSD of Gaussian monocycle pulses and the FCC spectral masks. b) 2nd order Gaussian monocycle pulse t_p=2.5ns.

input geometry to the physical channel model for a single path UWB channel is shown in Fig. 2. The propagation mechanisms for paths 1 and 3 are diffraction through the transmitter aperture and reflection, respectively. Consider single path impulse response $h(t)$, i.e. L=1 in (1). The magnitude of the frequency response $|H(f)|$ for path 3 in Fig. 2 is plotted in Fig. 3(a) for reflectors of various sizes and receiver located at position (10, 20). In this paper, we only consider flat reflectors. We observe that the magnitude response $|H(f)| \approx C f^{\alpha}$, where C is a constant and $\alpha > 0$ decreases as reflector size increases. For very small reflectors (size less than 1m) $\alpha \approx 0.5$, while for large reflectors (size greater than 10m) $\alpha \approx 0$.

Fig. 3(b) shows the magnitudes of the frequency responses as the receiver moves along line A in Fig. 2, and the reflector is absent. In this case $|H(f)| \approx C f^{\alpha}$, $\alpha < 0$ with $\alpha \approx -0.5$ for deep shadowing, i.e. for receiver positions to the left of (10,20) on line A in Fig. 2. As the receiver approaches the LOS region, the value of α tends to 0.

Given the transmit signal $p_t(t)$ with the Fourier transform $P_t(f)$, the output of the channel in frequency domain is $P_r(f) = H(f)P_t(f)$. Therefore, $|P_r(f)| \approx C f^{\alpha} |P_t(f)|$

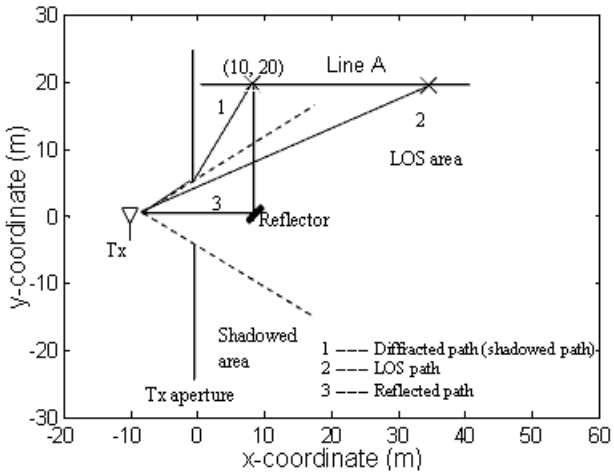

Figure 2. A simple geometry for the UWB physical model.

with $\alpha > 0$ for reflection and $\alpha < 0$ for diffraction. Note that $(j2\pi f)^{\alpha} P_t(f)$ is the Fourier transform of the fractional derivative operator [19,20] (also referred to as the fractional integral for $\alpha<0$), which reduces to the derivative for $\alpha=1$ and the integral for $\alpha=-1$. Thus, we employ per-path correlation templates given by the fractional derivatives of the transmit pulse

$$D^{\alpha} p_t(t) = F^{-1}((j2\pi f)^{\alpha} P_t(f)), \quad (7)$$

where F^{-1} is the inverse Fourier transform.

In Fig. 4, fractional integrals are utilized as templates for several diffraction paths along line A in Fig. 2 (see also Fig. 3(b)). For the 2nd order Gaussian monocycles in Fig. 1(a), per-path distortion is higher for t_p=0.25ns than for t_p=2.5ns since in this case higher frequencies are attenuated more due to diffraction. Thus, we choose the signal with t_p=0.25ns as the transmit pulse in Fig. 4. At each receiver position, we plot the SNR capture (5) for per-path correlation templates generated by varying the order of fractional integration α from -1 to 0 in (7). At location (5,20) the receiver is in the region of deep shadowing, and diffraction is the dominant propagation mechanism. In this case, the peak energy capture is achieved for α=-0.5 (semi-integral) correlation template since it closely matches the deep shadowing curve in Fig. 3(b). The loss in SNR capture when the transmit pulse $p_t(t)$ (α=0) and it's integral $\int p_t(t)dt$ (α=-1) are employed as templates is less than 0.5 dB. As the receiver moves towards the LOS region, diffraction-induced distortion becomes less severe, and the performance of transmit pulse $p_t(t)$ as correlation template improves: at position (25,20), its SNR capture approaches one while at the boundary between shadowed and LOS region at (30,20), the transmit pulse is the optimal template. We have also investigated template design for reflection-induced per-path distortion [16]. In this case, the worst case distortion occurs for the

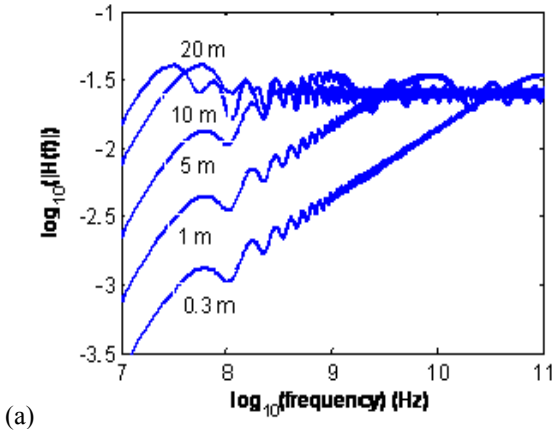

(a)

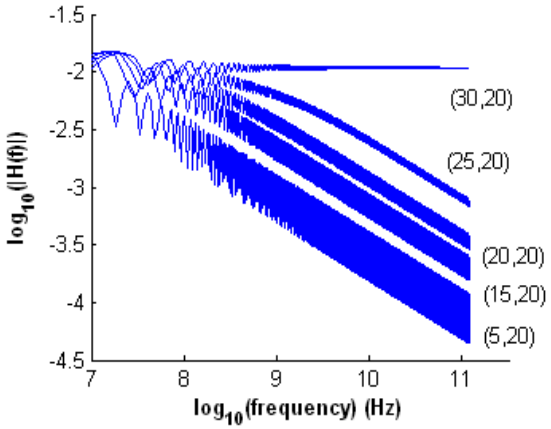

(b)

Figure 3. Amplitudes of frequency responses for paths in Fig. 2. (a) Path 3, reflectors of various sizes, receiver position at (10, 20) (b) Diffraction path for receiver positions along line A.

2nd order Gaussian monocycle with t_p=2.5ns. For path 3 in Fig. 2, the semi-derivative (α=0.5) is a near-optimal template for reflectors of small size (less than 3m), while the transmit pulse is the optimal template for medium-to-large sized reflectors (greater than 3m).

From the above results, we conclude that the semi-integral and the semi-derivative of the transmit pulse shape represent near-optimal templates in terms of SNR capture for the per-path distortion caused by deep shadowing and reflection by small reflectors, respectively. The loss in SNR capture when the transmit pulse $p_t(t)$ is employed as template is less than 0.5dB of the ideal template in this region while the transmit pulse is the optimal template choice for mild shadowing or reflection from large reflectors. When the higher order transmit pulses (e.g. the 8th order Gaussian monocycle in Fig. 1) are employed, the loss in SNR capture reduces considerably due to the high cross-correlations among their fractional derivatives of various orders [16]. Thus, the transmit pulse is a simple but robust template choice in practical UWB systems [1, 7].

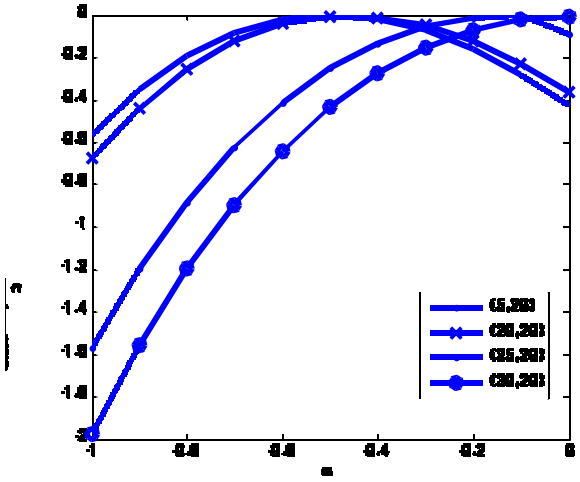

Figure 4. SNR_c capture for fractional integral templates of order α for receiver positions along line A in Fig. 2 (diffraction to LOS), 2nd Gaussian monocycle t_p=0.25ns transmit pulse.

IV. TEMPLATE DESIGN FOR MULTIPATH CHANNELS.

A. *Channel Model and Receiver Design*

A physical model scenario Fig. 5(a) is employed to test template design for outdoor multipath UWB channels. The received signal contains more than 20 multipath components, which are due to small reflectors (less than 3m) and shadowing. For the receiver position (12, 15), reflection is the dominant propagation mechanism due to the direct (specular) reflection at this position [7,21,16]. At (3, 15), direct reflections are not present due to the orientation of the reflectors, and the received signal is made up of multipath components diffracted from the edges of the reflectors and the aperture. At this location diffraction is the dominant propagation mechanism as illustrated in 5(b).

Several approaches to transmitter [22] and receiver [3,23] design have been proposed. In this paper, we employ the iterative receiver described in [3]. For the kth iteration, the location of the peak of the correlation between the template waveform and the received signal determines the estimated arrival time $\hat{\tau}_k$ of the kth multipath component, and the received energy at the output of this correlator is used to estimate the channel attenuation for that component. The template, scaled by this estimate, is then subtracted from the received signal, and the next iteration is performed, until a predetermined number of paths are captured.

Since the fractional derivative templates are near-optimal for single path channels as discussed in section III, we employ them as per-path templates for the iterative receiver in multipath scenarios. Multiple waveforms are employed in each iteration, and the waveform that produces the highest correlation is selected as the template.

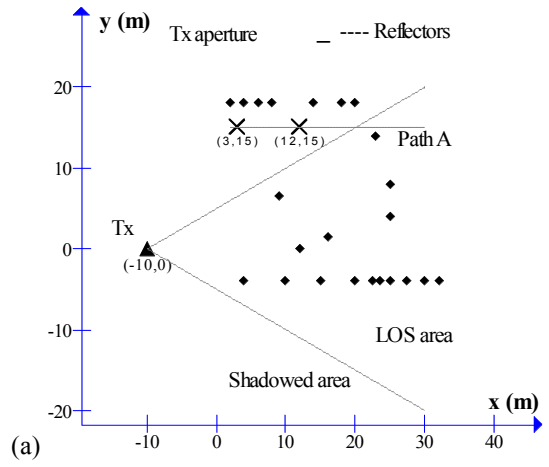

(a)

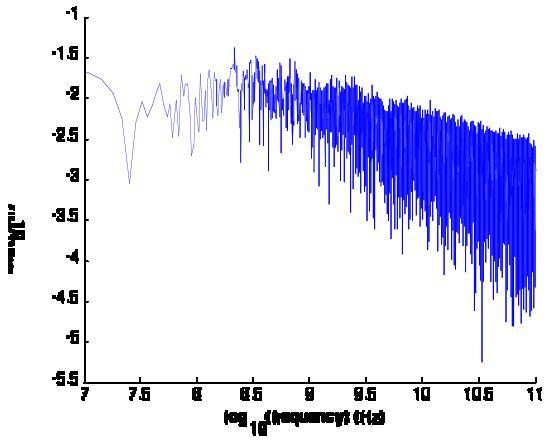

(b).

Figure 5. (a) Sample geometry for an outdoor multipath channel. (b) Magnitude response of multipath UWB channel at receiver location (3, 15) in (a) (diffraction-dominated scenario).

Three suboptimal receivers are investigated, distinguished by the sets of templates employed in each iteration: (i) 1 template (the transmit pulse); (ii) 3 templates (the transmit pulse, its semi-integral (α=-0.5), and semi-derivative (α=0.5)); (iii) 11 templates (the transmit pulse and the fractional derivatives waveforms with uniformly spaced α in the interval [-0.5, 0.5]). Note that these values of α span the range of dominant propagation mechanisms from deep shadowing to LOS to reflection by small reflectors. Here α=0.5 and α=-0.5 denote the optimal templates for worst case distortion caused by reflection from small reflectors and deep shadowing, respectively. Thus, iterative receivers (ii) and (iii) are robust to frequency-dependent distortion and are simple to implement since the knowledge of the propagation mechanism is not required at the receiver. Finally, we employ the transmitted reference template [24] in simulations to provide an upper bound on the SNR capture.

B. Template design for channels with interpulse interference (IPI)

While template design for multipath channels with non-overlapping multipath components is a straightforward extension of the single path case, the IPI results in additional distortion that can affect template design. IPI occurs when the difference between the times-of-arrival of several multipath components is less than the pulse width of the transmit pulse selected for UWB transmission. For outdoor UWB channels, IPI can occur due to a group of closely spaced reflectors (scatterers), diffraction of pulses from the edges of a reflector or from ground bounce where the LOS multipath component overlaps with the component reflected from the ground. For simplicity and without loss of generality, we assume that IPI occurs between two arriving multipath components at the receiver, but it will be clear that our proposed method of template design is applicable for IPI among multiple pulses. Since pulses in the lower band of the UWB mask are more susceptible to IPI than pulses in the upper band due to larger pulse width, we employ the 2nd

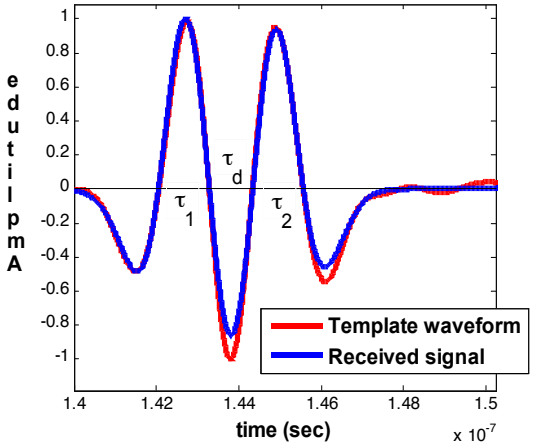

(a)

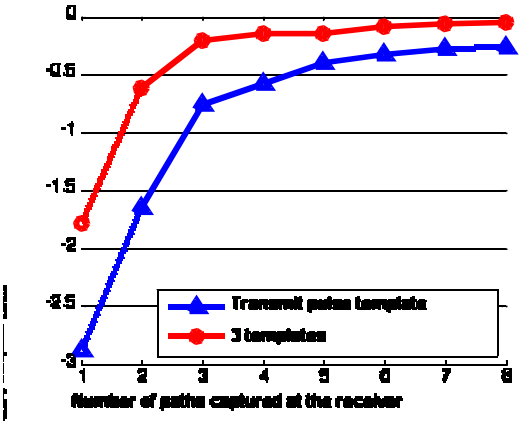

(b)

Figure 6. (a) Received signal and template waveform for two overlapping pulses. (b) SNR capture vs. number of paths employed at the receiver for signal in (a).

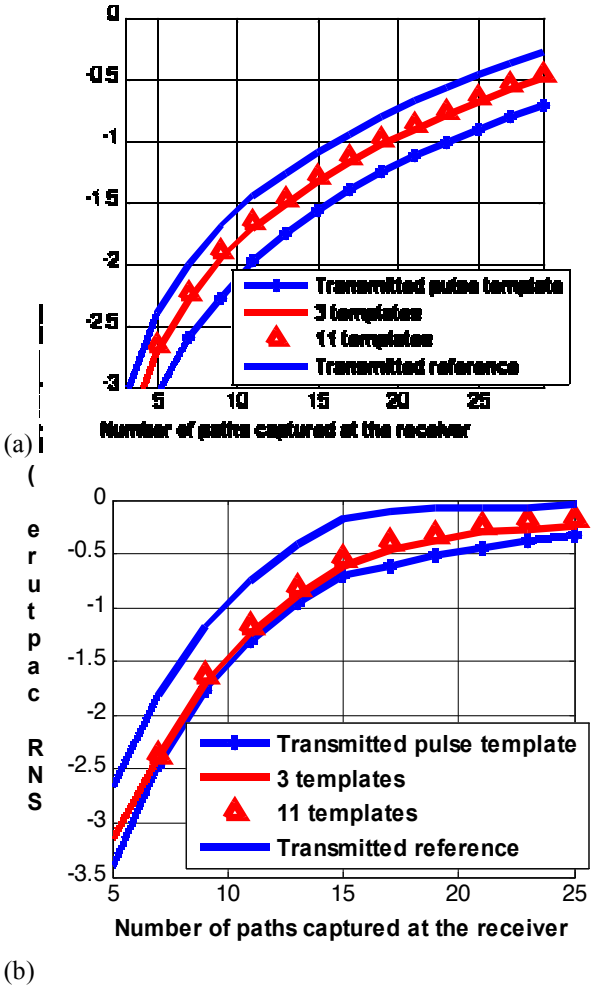

Figure 7. SNR capture as a function of the number of paths captured at the receiver position (3,15). Diffraction is the dominant propagation mechanism; 2nd order Gaussian monocycle transmit pulses: a) t_p=0.25ns b) t_p=2.5ns

order Gaussian monocycle pulse with t_p=2.5ns illustrated in Fig. 1(b) in the numerical results below.

Fig. 6(a) illustrates the IPI between two received multipath pulses (e.g. due to a ground bounce) with individual times-of-arrival at τ_1=143ns and τ_2=145ns when a single UWB pulse is transmitted. We observe that the received signal affected by IPI can be approximated by a sum of fractional derivatives of the transmit pulse for various α and time shifts, and the dominant component is at τ_d=143.9ns for the IPI illustrated in Fig. 6(a). Thus, a simple approach to iterative receiver design is to employ more than two iterations to capture sufficient energy from the received signal. For example, in Fig. 6(a), the first three iterations correspond to the times of arrival τ_d, τ_1 and τ_2, respectively. Note the resulting weighted sum of templates closely matches the received waveform. In Fig. 6(b), we plot the SNR capture vs. the number of iterations for the received signal in Fig. 6(a). We observe that capturing only two paths results in more than 1dB loss in SNR capture. As the number of iterations increase, the SNR capture improves significantly. The receiver that chooses from three templates at each iteration achieves near-optimal SNR capture after just three iterations.

C. Template design for multipath UWB channels with per-path distortion.

We investigated SNR capture (5) of proposed receivers for multipath channels affected by diffraction and reflection by small reflectors [16]. Fig. 7 shows the SNR capture vs. the number of paths L' captured by the iterative receiver when the receiver is at location (3, 15) (see Fig. 5), and the dominant propagation mechanism is diffraction from the edges of the reflectors and the transmitter aperture. Since higher frequencies are attenuated in this case, employing multiple templates at each iteration is more beneficial for the pulse with t_p=0.25ns in Fig. 7(a) than for the pulse with t_p=2.5ns in Fig. 7(b), where the receiver that employs single transmit pulse template suffers relatively small performance degradation as compared to the fractional derivatives templates. We also observe that the receiver that employs just three templates has a very small loss (less than 0.2 dB) in SNR capture as compared to the transmitted reference receiver restricted to the duration specified by the number of paths. This example and results in [16] illustrate that using fractional derivatives/integrals as templates provides near-optimal performance while simple iterative receiver based on the transmit pulse provides excellent complexity-performance trade-off for practical multipath outdoor scenarios.

We also observe that approximately twice as many paths are required for the pulse with t_p=0.25ns than for the pulse with t_p=2.5ns to attain a particular value of SNR capture. This is due to the fact that the received multipath components arrive after undergoing diffraction from the two edges of that reflector/aperture since direct reflection is absent in this case. When the difference in the arrival time of these two multipath components is greater than the transmit pulse width (e.g. for the pulse with t_p=0.25ns in Fig. 7(a)), they resolve completely at the receiver, and two separate iterations are required to capture their energy. On the other hand, the signals diffracted from the two edges overlap when the transmit pulse width is longer (e.g. for the pulse with t_p=2.5ns in Fig. 7(b)). Although the wider pulse is more susceptible to IPI, the number of iterations required to approach desired SNR capture for this pulse is smaller than for the shorter pulse in Fig. 7(a).

V. PROPAGATION GAIN COMPARISON

The propagation gain (PG) is defined as the ratio of the received and transmitted signal energies [7]:

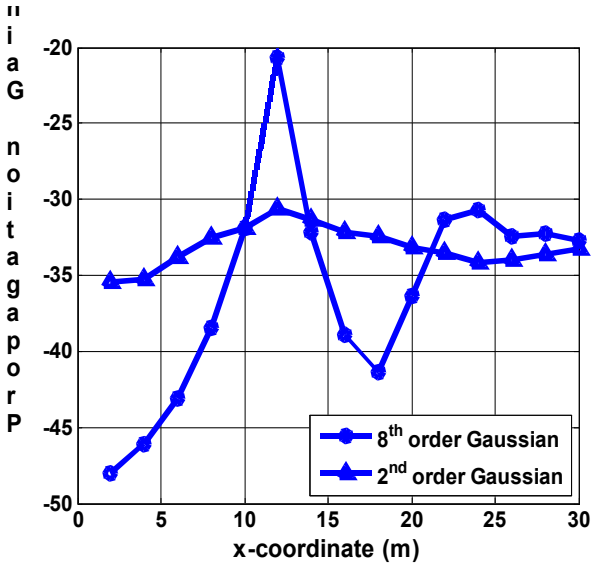

Figure 8. Comparison of propagation gain for the Gaussian monocycle pulses in Fig. 1 as the receiver moves along line A in Fig 5.

$$PG = \int_{-\infty}^{\infty} p_r^2(t)dt \Big/ \int_{-\infty}^{\infty} p_t^2(t)dt. \qquad (8)$$

As discussed in [7], the PG depends strongly on the propagation mechanism and the frequency band occupied by the transmit pulse within the UWB spectrum. In Fig. 8, we compare frequency and position-dependent propagation gain for the 2nd (t_p=2.5ns) and 8th (t_p=0.25ns) order Gaussian monocycles as the receiver moves along line A in Fig. 5. The spectra of these pulses reside in the lower (0-0.96 GHz) and upper (3.1-10.6 GHz) bands of the FCC spectral mask, respectively (see Fig. 1). Note that the upper band pulse is about 10dB stronger than the lower band pulse at position (12,15) where the dominant propagation mechanism is direct reflection from small reflectors. The PG of this signal in the non-LOS region depends strongly on the presence of specular reflection in given location [21]. On the other hand, the lower band pulse is more robust and maintains its gain in the diffraction-dominated scenario (e.g. at (3,15)), with over 10dB advantage over the upper band pulse.

From these results and [7], we conclude that exploiting lower band pulses can be beneficial in practical UWB systems. These conclusions motivate development of adaptive UWB transmission methods that select pulses in either the lower or upper band depending on the dominant propagation mechanism.

VI. CONCLUSION

The UWB physical model was used to investigate per-path distortion and robust template design for scenarios affected by diffraction and reflection by small reflectors. Near-optimal SNR capture was demonstrated using fractional derivatives per-path templates in multipath channels with inter-pulse interference for dominant outdoor propagation mechanisms. Comparison of the propagation gain demonstrated benefits of utilizing transmit pulses in the lower and upper bands of the FCC mask in environments dominated by diffraction and reflection, respectively.

REFERENCES

[1] M. Z. Win and R. A. Scholtz, "Impulse radio: how it works," IEEE Commun. Lett., vol. 2, no. 2, pp 36-38, 1998.
[2] Federal Communications Commission, "First Report and Order, Revision of Part 15 of the Commission's Rules Regarding Ultra Wideband Transmission Systems," ET Docket 98-153, Feb. 14, 2002.
[3] R. D. Wilson, R. A. Scholtz, "Template Estimation in Ultra-Wideband Radio," Record of the 37th Asilomar Conference, Nov. 2003.
[4] A. Taha and K. M. Chugg, "On designing the optimal template waveform for UWB impulse radio in the presence of multipath," in IEEE Conference on Ultra Wideband Systems and Technologies, pp 41-45, 2002.
[5] R. C. Qiu, "A Study of the Ultra-wideband wireless propagation channel and optimum UWB receiver design," IEEE JSAC, Vol. 20, No. 9, pp. 1628-1637, Dec. 2002.
[6] R.C. Qiu, "Physics-based Generalized Multipath Model and Optimum Receiver Structure", in Design and Analysis of Wireless Networks, Nova Science Publishers, 2004.
[7] Li Ma, A. Duel-Hallen, Hans Hallen, "Physical modeling and template design for UWB channels with per-path distortion," Proc. of MILCOM 2006.
[8] H. Hallen, A. Duel-Hallen, S. Hu, T. S. Yang, M. Lei, "A Physical Model for Wireless Channels to provide Insights for Long Range Prediction", Proc. of MILCOM'02, Oct 7-10, 2002.
[9] R. D. Guenther, Modern Optics, New York: Wiley, 1990.
[10] L. B. Felsen and N. Marcuvitz, Radiation and Scattering of Waves, Prentice-Hall, 1973.
[11] S. Zhao and H. Liu, "On the Optimum linear receiver for impulse radio system in the presence of overlapping," IEEE Comm. Lett., vol. 9, pp. 340-342, Mar. 2005.
[12] S. Zhao and H. Liu, "Prerake Diversity Combining for Pulsed UWB Systems considering Realistic Channels with Pulse Overlapping and Narrow-Band Interference," Proc. GLOBECOM 2005., vol. 6.
[13] T. S. Rappaport, Wireless Communications, Prentice-Hall, 1996.
[14] R.A. Scholtz, "Multiple Access with Time Hopping Impulse Modulation," Proc. MILCOM'93, Dec. 1993, pp. 447-450.
[15] J. G. Proakis, Digital Communications, 4th ed., McGraw Hill, 2001
[16] N. Mehta, "Analysis of multipath UWB channels for efficient receiver template design," MS Thesis, NC State University, Aug. 2008
[17] J. Zhang, T. D. Abhayapala and R. A. Kennedy, "Performance of Ultra-wideband Correlator Receiver Using Gaussian Monocycles," in Proc. IEEE ICC 2003.
[18] Y. Zhang, A.K.Brown, "Complex multipath effects in UWB communication channels", IEE Proc.-Comm., vol. 153, no. 1, pp 120-126, Feb. 2006
[19] R. C. Qiu, C. Zhou, and Q. Liu, "Physics-based pulse distortion for ultra-wideband signals," IEEE Trans. Veh. Technol.,vol. 54, no. 5, pp. 1546-1555, Sep. 2005.
[20] K.S.Miller, B. Ross, An introduction to the fractional calculus and fractional differential equations, John Wiley & Sons, 1993
[21] L. Ma, "Investigation of transmission, propagation and detection of UWB pulses using physical modeling," Ph.D. Dissertation, NC State University, Dec. 2006.

[22] K. Usuda, H. Zhang, M. Nakagawa, "Pre-Rake performance for pulse-based UWB system in a standardized UWB short-ranged channel," Proc. IEEE WCNC'04, vol. 2, Mar. 2004.
[23]M. Z. Win and R. A. Scholtz, "On the Energy Capture of Ultrawide Bandwidth Signals in Dense Multipath Environments", IEEE Comm. Lett., vol. 2, no. 9, pp. 245-247, Sep. 1998.
[24] R. T. Hoctor and H. W. Tomlinson, "An overview of delay-hopped transmitted-reference RF communications", Technique Information Series: G.E Research and Development Center, Jan. 2002.